

Experimental and DFT Computational Insight into Nitrosamine Photochemistry—Oxygen Matters

Ashwini A. Ghogare,^{†,‡} Ciro J. Debaz,[†] Marilene Silva Oliveira,^{†,§} Inna Abramova,[†] Prabhu P. Mohapatra,[†] Kitae Kwon,^{||} Edyta M. Greer,^{*,||} Fernanda Manso Prado,[§] Hellen Paula Valerio,[§] Paolo Di Mascio,^{*,§} and Alexander Greer^{*,†,‡,||}

[†]Department of Chemistry, Brooklyn College, 2900 Bedford Avenue, Brooklyn, New York 11210, United States

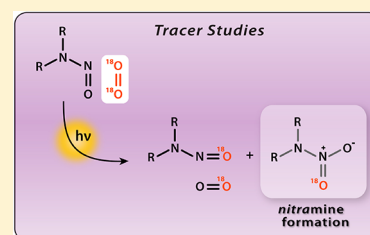
[‡]Ph.D. Program in Chemistry, The Graduate Center of the City University of New York, 365 Fifth Avenue, New York, New York 10016, United States

[§]Departamento de Bioquímica, Instituto de Química, Universidade de São Paulo, CEP, 05508-000 São Paulo, Brazil

^{||}Department of Natural Sciences, Baruch College, City University of New York, New York 10010, United States

Supporting Information

ABSTRACT: A nitrosamine photooxidation reaction is shown to generate a peroxy intermediate by experimental physical-organic methods. The irradiation of phenyl and methyl-substituted nitrosamines in the presence of isotopically labeled 18-oxygen revealed that an O atom was trapped in a peroxy intermediate to trimethylphosphite or triphenylphosphine, or by nitrosamine itself, forming two moles of nitramine. The unstable peroxy intermediate can be trapped at low temperature in postphotolyzed solution in the dark. Chemiluminescence was also observed upon thermal decomposition of the peroxy intermediate, that is, when a postphotolysis low-temperature solution is brought up to room temperature. A DFT study provides tentative information for cyclic nitrogen peroxide species on the reaction surface.



1. INTRODUCTION

Nitrosamines are carcinogenic substances, but current research can look beyond their known role as biological alkylating agents.¹ Nitrosamine studies have focused on sunlight photolysis,² Fenton reactions,³ or treatment with ozone,^{4,5} hydroxyl radicals, or hydrated electrons^{6,7} that lead to amines via denitrosation (i.e., loss of NO[•]) (Figure 1).^{8,9}

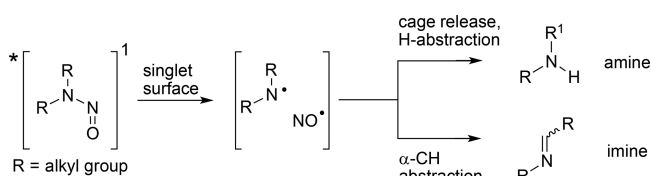


Figure 1. Nitrosamine photodenitrosation and formation of amines and imines; the latter is involved in a rebound reaction to abstract H at the α -C–H group. This result is from previous literature (refs 14 and 15).

Except for a paper in 2015,¹⁰ there is no previous literature that describes distinct photochemistry of nitrosamines in the presence of oxygen. Figure 2 shows a reaction from the 2015 paper¹⁰ of an internal nitrosamine-to-molecular oxygen ¹⁸O scrambling reaction (in general, oxygen isotopes can aid in studying mechanisms for reactive intermediates that are difficult to isolate^{21–29}), but there is a need for determining whether

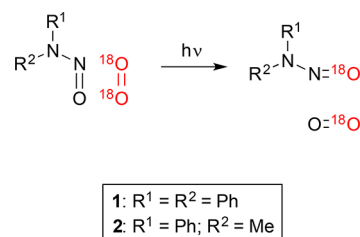


Figure 2. An O atom from an incoming O₂ can displace the nitroso O and generate the same compound but with an ¹⁸O label. This result is from previous literature (ref 10).

external O atom transfer and trapping reactions occur in nitrosamine photooxidations.

The 2015 paper was a preliminary study¹⁰ that implied the existence of a peroxy intermediate, but no O atom transfer to trapping compounds was noted. In the current study, we hypothesized that oxygen isotopes and trapping reactions will demonstrate the formation of a peroxy intermediate in nitrosamine photooxidation. The specific aim of the current research was to determine whether O-transfer arises from intermediates generated in the UV photolysis of nitrosamines.

Received: March 14, 2017

Revised: July 13, 2017

Published: July 14, 2017



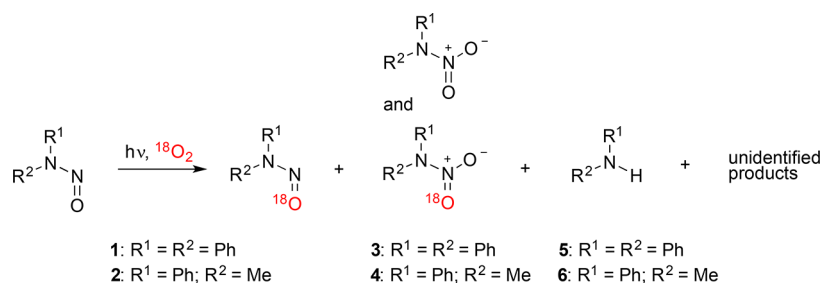


Figure 3. New results showing oxygen atom is incorporated into nitrosamines **1** and **2**, or is transferred to form nitramine products **3** and **4**. A doubly ¹⁸O-labeled nitramine [R²R¹NN(= ¹⁸O)¹⁸O] was not observed. The O-transfer chemistry results from the intermediacy of a peroxy species, where the radicals also produce products, including amines **5** and **6**.

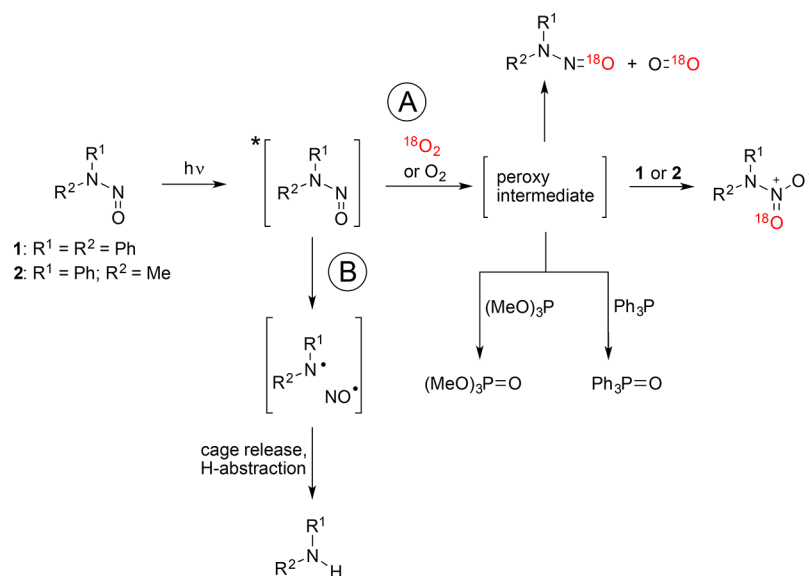


Figure 4. New proposed mechanism where (A) O₂ adds to excited state nitrosamine to form a peroxy intermediate. The peroxy intermediate transfers an oxygen atom to a phosphite trap or phosphine trap or into nitrosamine and forms the nitramine product or can release dioxygen with ¹⁸O-label scrambling. (B) An excited nitrosamine leads to the loss of NO[•] and forms an aminyl radical in a competitive process with path A.

Previous literature of the anaerobic photochemistry of nitrosamines can be summarized in 4 points (i) literature was focused on NO[•] expulsion reactions.^{11–20} Early nitrosamine photochemistry work can be traced back to Chow et al.^{11–15} who used N₂-degassed conditions. (ii) Anaerobic conditions yielded aminyl radicals from the photolysis of aliphatic nitrosamines. (iii) Flash photolysis and ESR studies of aliphatic nitrosamines under anaerobic conditions were reported, where the absence of O₂ gave a clearer view of R₂N[•] and NO[•] radicals.^{11–15} (iv) Imines are also known to arise from the H atom abstraction of α-C–H groups in a rebound reaction by the aminyl radical, R₂N[•]. We view Chow's nitrosamine photochemistry under anaerobic conditions as a forerunner to our nitrosamine photooxidation work described in this report. To reiterate, O-transfer processes such as trapping and the generation of nitramines **3** and **4** have not been reported.

In the current study, we report the first trapping of a peroxy intermediate in nitrosamine photooxidation. A peroxy oxygen is diverted to substrate in a self-oxidation to give nitramines **3** and **4** (Figures 3). As we will see, flowing ¹⁸O₂ gas in and tracing ¹⁸O-labeled compounds out offer new mechanistic insights. Phosphite and phosphine traps for O atom transfer along with chemiluminescence data, and DFT calculations have also provided insight. Evidence has been collected that supports

the mechanism depicted in Figure 4A for peroxy intermediate formation and in Figure 4B for aminyl radical formation.

2. METHODS

Reagents and Instrumentation. *N,N*-Diphenylnitrosamide **1**, *N*-methyl-*N*-phenylnitrosamide **2**, diphenylamine **5**, *N*-methylaniline **6**, trimethylphosphite, trimethylphosphate, triphenylphosphine, CH₃CN, CD₃CN, CHCl₃, CDCl₃, toluene, and ¹⁸O₂ gas (99% ¹⁸O) were purchased from commercial suppliers. Caution is required because nitrosamines are carcinogenic. Nitrosamines **1** or **2** were irradiated with a pair of 400 W metal halide lamps (λ > 280 nm) or with a 254 nm UV pen light (Heraeus UV lamp). Electrospray ionization mass data were collected in a positive ion mode with direct sample introduction to the instrument. MS/MS data were collected using a mass spectrometer and an electrospray ionization tandem unit equipped with an LC18-S column. HPLC/MS data were collected using a C18 column (150 mm × 3.9 mm) in 90% acetonitrile in water, UV–visible detection at 280 nm, +ESI detector, and a fragment voltage of 175. MassLynx 1.4 software³⁰ allowed the calculation of isotopomers and their natural abundance. A GC/MS instrument was also used. Proton NMR spectra were collected at 400 MHz.

Synthesis of *N,N*-Diphenylnitramide **3.** Compound **3** was synthesized from diphenylamine using the procedure of

Daszkiewicz et al.³¹ Structural identification of **3** was carried out by IR, NMR, and mass spectroscopy, and the HPLC data indicated a purity of 98%. HRMS (+ESI) calcd for $C_{12}H_{11}N_2O_2$ = 215.0821, obtained m/z = 215.0820. IR (neat): 875 cm^{-1} (N–O stretch), 1285, 1529 cm^{-1} (NO₂ stretching frequencies), 2880, 2941, 2970 cm^{-1} (aliphatic C–H stretching vibrations). ¹H NMR (400 MHz, CD₃CN) δ 7.49–7.51 (m, 8H), 7.43–7.46 (m, 2H).

Photooxygen Exchange and Transfer Reactions.

Nitrosamines **1** or **2** were irradiated under O₂ saturation. A typical experiment contained nitrosamines **1** or **2** (1 mM) in 1 mL of ¹⁸O₂-saturated CHCl₃, CDCl₃, or CH₃CN in a vial (3 mL) or an NMR tube at 25 °C. The results were the same using chloroform or acetonitrile solutions. Two different methods were used to sparge solutions with ¹⁸O₂. *Condition A*: Liquid N₂ was used to freeze and thaw solutions while under vacuum, after which a connection was made to the ¹⁸O₂ cylinder, and the system was sealed during irradiation. *Condition B*: Solutions were flushed with N₂, followed by ¹⁸O₂. Samples were typically irradiated for 1 h and flushed again with ¹⁸O₂ gas after 30 min periods.

¹⁸O-Labeled and Unlabeled *N,N*-Diphenylnitrous Amide (**1**) and *N,N*-Diphenylnitramide (**3**), and Diphenylamine (**5**). MS/MS peaks showed **1** (m/z = 199) and ¹⁸O-labeled **1** (m/z = 201) both at 24.69 min, **3** (m/z = 215) and ¹⁸O-exchanged **3** (m/z = 217) at 25.53 min, and Ph₂NH (**5**) (m/z = 170) at 26.51 min. HPLC/MS: t_R = 5.49 min; HRMS (+ESI) calcd unlabeled $C_{12}H_{11}N_2O$ **1** = 199.0871, found 199.0872; calcd for labeled $C_{12}H_{11}N_2^{18}O$ **1** = 201.0938, found 201.0958. HRMS (+ESI) calcd unlabeled $C_{12}H_{11}N_2O_2$ **3** = 215.0821, found 215.0820; calcd for labeled $C_{12}H_{11}N_2^{18}O^{16}O$ **3** = 217.0876, found 217.0929. We previously reported the detection of ¹⁸O-labeled nitrosamine **1** and Ph₂NH **5**.¹⁰

¹⁸O-Labeled and Unlabeled *N,N*-Methyl-*N*-phenylnitrous Amide (**2**) and *N*-Methylaniline, *N*-Methyl-*N*-phenylnitramide (**4**), and *N*-Methylaniline (**6**). MS/MS spectra show peaks for **2** (m/z = 137) and ¹⁸O-labeled **2** (m/z = 139) at 12.69 min, **4** (m/z = 153) and ¹⁸O-labeled **4** (m/z = 155) at 13.94 min, and **6** (m/z = 108) at 4.81 min. HPLC/MS: t_R = 3.92 min; HRMS (+ESI) calcd unlabeled $C_7H_9N_2O$ **2** = 137.0715, found 137.0724; calcd for labeled $C_7H_9N_2^{18}O$ **2** = 139.0757, found 139.0755. We previously reported the detection of ¹⁸O-labeled nitrosamine **2** and methylaniline **6**.¹⁰

Detection of Diphenylanthracene (DPA) Endoperoxides by Mass Spectrometry. Mass spectrometry analyses of DPA endoperoxides were carried out in a UHR-APCI-Q-TOF Bruker Daltonics MaXis 3G spectrometer (Bruker, Billerica, MA, U.S.A.) coupled to a 1200 Shimadzu HPLC system CBM-20A (Tokyo, Japan). DPA¹⁶O₂, DPA¹⁸O₂, and DPA¹⁶O¹⁸O were detected using an Atmospheric Pressure Chemical Ionization (APCI) source in the positive mode. Supelcosil (5 μ m C18 150 \times 4.6 mm i.d) column was used at 25 °C with solvent A (0.1% formic acid) and solvent B (acetonitrile) with a flow rate of 0.8 mL/min. The linear gradient used was as follows: 30% B at 0 min, 100% B at 10 min, 100% B at 20 min, 30% B at 22 min, 30% B at 30 min. The APCI conditions were the following: capillary, 4.5 kV; corona, 3.5 kV; end plate, 500 V, dry heater, 180 °C; APCI heater, 300 °C, nebulizer 2.5 bar, dry gas, 5.0 L/min. Nitrogen was used as collision gas, and collision energy used for all precursor ions was 10 eV.

In Situ Trapping Reactions with Trimethylphosphite.

Trapping studies were conducted in 700 μ L of O₂-saturated CDCl₃ of **1** (20–60 mM) containing various concentrations of (MeO)₃P at 27 °C. ¹⁶O₂ or ¹⁸O₂ gas was flushed through the reaction mixtures prior to photolysis, and at 30 min intervals, the samples were flushed again with ¹⁶O₂ or ¹⁸O₂ gas for 3 min. Concentrations of (MeO)₃P and (MeO)₃P=O were determined by ¹H NMR with added toluene as the internal standard. HRMS (+ESI) calcd unlabeled $C_3H_{10}PO_4$ = 141.0317, found 141.0311; calcd labeled $C_3H_{10}P^{18}O^{16}O_3$ = 143.0359, found 143.0352.

Postphotolysis Trapping Reactions with Triphenylphosphine. Nitrosamine **1** (1 mM) was irradiated with the 254 nm UV pen light inserted into a 5.9 mL O₂-saturated CH₂Cl₂ solution for 30 min at –90 °C. By the end of the 30 min, the temperature had increased to –70 °C. Afterward, in the dark, PPh₃ (0.5 mM) was added to the solution and stirred for ~5 min, where Ph₃P=O was detected by GCMS. Biphenyl was used as the internal standard.

Chemiluminescence Measurements. A 10 mL CH₂Cl₂ solution of nitrosamine **1** (4.8 mM) was irradiated for 5 min inside a glass Corex tube using a UV pen light in solution at –72 °C (dry ice and ethanol). A Teflon tube was inserted into the solution for the bubbling of oxygen or nitrogen. The samples were prepared in (i) O₂-saturated CH₂Cl₂, (ii) N₂-saturated CH₂Cl₂, and (iii) O₂-saturated CH₂Cl₂ where 9,10-diphenylanthracene (100 mM) was added to the reaction after the photolysis. In the dark, immediately after the irradiation, the tube was transferred to a cuvette holder inside the photon counter system. The light emission was immediately recorded using a FLSP 920 photon counter (Edinburgh Instruments, Edinburgh, U.K.) consisting of two UV–visible Hamamatsu detectors R9110, maintained at –20 °C using a CO1 thermoelectric cooler also purchased from Edinburgh Instruments. During the chemiluminescence measurement, the temperature of the solution was increased from –72 to 22 °C.

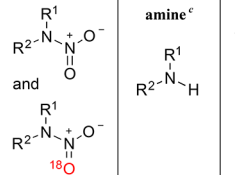
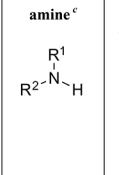
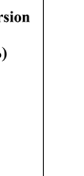
Computational Details. All of the calculations were performed with Gaussian 09 (revision D.01)³² at the ω b97x-D functional³³ and the 6-311+G(d,p) basis set, on the singlet surface in gas phase, and were visualized with GaussView 5.0.³⁴ For calculations involving nitroxide species, the unrestricted ω b97x-D functional was used to account for its diradical nature. Unrestricted functional was also used to calculate the radical rearrangement. These levels of theory were used in our previous study involving nitrosamine,¹⁰ and have been shown to work well in singlet oxygen calculations.³⁵ Frequency calculations were performed in order to confirm the natures of all minima (all positive eigenvalues in the Hessian) and first-order saddle points (one negative eigenvalue in the Hessian). The first-order saddle points were verified with intrinsic reaction coordinate calculations.^{36,37} For these DFT calculations, extra quadratic convergence for self-consistent field method (scf = xqc) and ultrafine integral (int = grid = ultrafine) facilitated the convergence of all geometries. For all the calculations involving the unrestricted method, command “guess = (mix,always)” was used for the broken symmetry wave function. The energies provided are the sum of electronic energy and thermal energy at 298.15 K. Time-dependent density functional theory (TD-DFT) calculations of vertically excited singlet (S_1) and triplet states (T_1) were carried out with ω b97x-D/6-311+G(d,p), using the optimized singlet ground state (S_0) structures of **1** and **B**. Because of potential triplet (T_1) instabilities,³⁸ the TD-DFT calculations were used with

the Tamm–Dancoff approximation (TDA).³⁹ All diradical compounds were calculated with triplet broken symmetry solutions.

3. RESULTS AND DISCUSSION

Photolysis of Nitrosamines 1 and 2 in the Presence of ¹⁸O₂ or ¹⁶O₂. Table 1 shows that ¹⁸O was exchanged with ¹⁶O.

Table 1. Products Formed Upon UV Irradiation of Nitrosamines 1 and 2 in the Presence of ¹⁸O₂

nitrosamine	% yield of photoproducts for nitrosamine after 3-h irradiation ^a				percent conversion (%)
	¹⁸ O-labeled nitrosamine ^{b,c}	nitramine (¹⁶ O + ¹⁸ O) ^b	amine ^c	unidentified products	
 1 (<i>m/z</i> = 199)	8±2 [(M+2)+H] ⁺ = 201	 4±2	17±2 [M+H] ⁺ = 170	6±2	35±4
 2 (<i>m/z</i> = 137)	12±3 [(M+2)+H] ⁺ = 139	6±2	28±4 [M+H] ⁺ = 108	4±2	50±2

^aThe concentration of nitrosamines 1 or 2 was 5 mM in 1 mL CH₃CN, where the products were detected by HPLC/MS. Errors are shown as mean ± standard deviation. Control experiments demonstrate that H₂¹⁸O is inert to 1 and 2 in the presence of UV light in CH₃CN. ^bBased on the combined areas of peaks at [M + H]⁺ and [(M + 2) + H]⁺. ^cYields for ¹⁸O-labeled nitrosamines and amines were previously reported.¹⁰

and 2, and introduced into nitramines 3 and 4. Figures 5–7 show the mass data of 1 and 2 following UV irradiation for 3 h. The MS/MS peaks are shown in Figure 5 for 1 (*m/z* = 199) and ¹⁸O-labeled 1 (*m/z* = 201 [(M + 2) + H]⁺) both at 24.69 min, nitramine 3 (*m/z* = 215 (M + H)⁺) and ¹⁸O-labeled nitramine 3 (*m/z* = 217 [(M + 2) + H]⁺) both at 25.53 min, and Ph₂NH 5 (*m/z* = 170 (M + H)⁺, 26.51 min). Figure 6 shows the MS/MS peaks of unlabeled 2 (*m/z* = 137 (M + H)⁺) and ¹⁸O-labeled 2 (*m/z* = 139 [(M + 2) + H]⁺) both at 12.69 min, nitramine 4 (*m/z* = 153 (M + H)⁺) and ¹⁸O-labeled nitramine 4 (*m/z* = 155 [(M + 2) + H]⁺) both at 13.94 min, and amine 6 (*m/z* = 108 (M + H)⁺) at 4.81 min.

Our identification of nitramine 3 and amine 5 was also assisted by comparative analyses using synthesized or commercial samples; that is, spiking a synthesized sample of nitramine 3 increased the *m/z* = 215.0820 peak at 5.32 min, and spiking a commercial sample Ph₂NH 5 increased the *m/z* = 170.0963 peak at 5.71 min. It is worth noting that our mass determinations do not prove the structures. For example, a conceivable rearrangement pathway is from the diphenylaminyl radical to the biphenyl-2-aminyl radical. However, DFT calculations indicate a high barrier process $\Delta H^\ddagger = 61.9$ kcal/mol (Figures S2 and S3, Supporting Information) and offer an

explanation as to why the byproduct biphenyl-2-amine was not detected in the reaction. We note that our interpretation of reaction mixtures containing peroxide type compounds can be problematic because of possible rearrangements and reactions during ionization/spray processes while acquiring mass spectrometry data.

In the reaction mixture, amines were formed in 17–28% yields, as well as 4–6% of unidentified products. As ¹⁸O is exchanged in 1, ¹⁶O=¹⁸O gas is expelled into the solution as we will see next.

Photolysis of Nitrosamine 1 with ¹⁸O₂ Gas and Trapping of Expelled ¹⁶O=¹⁸O Gas. The photolysis of 1 (5 mM) was carried out in CH₂Cl₂ presaturated with ¹⁸O₂ gas at –72 °C in a sealed 4 mL quartz tube (diameter 1 cm). Some residual ¹⁶O₂ remained. A UV pen-light was used in an inner glass tube. After photolysis, the solution was brought up to a room temperature of 22 °C, and 9,10-diphenylanthracene (DPA, 5 mM) was added to the inside of the sealed quartz tube. Using a reported technique,⁴⁰ molecular oxygen (¹⁸O₂, ¹⁶O=¹⁸O and ¹⁶O₂) in the solution was trapped by irradiating with a 500 W tungsten lamp for 90 min where the DPA sensitized the formation of double labeled, mono labeled, and unlabeled singlet oxygen, detected as the DPA endoperoxides (DPA¹⁶O¹⁶O, DPA¹⁶O¹⁸O, and DPA¹⁸O¹⁸O). Figure 7 shows the HPLC traces and mass spectra of DPA¹⁶O¹⁶O, DPA¹⁶O¹⁸O, and DPA¹⁸O¹⁸O. Figure S4 (Supporting Information) shows the product ion mass spectrometry data for the DPA¹⁶O¹⁶O, DPA¹⁶O¹⁸O, and DPA¹⁸O¹⁸O endoperoxides.

Trapping of a Peroxy Intermediate with Trimethylphosphite [(MeO)₃P] in Situ. A plausible explanation for the generation of nitramines 3 and 4 is that the peroxy intermediate transfers an O atom to nitrosamines 1 and 2. Thus, O atom transfer of the peroxy intermediate to trapping agents trimethylphosphite, (MeO)₃P, and triphenylphosphine, Ph₃P, were investigated next. Phosphites have been reported as in situ trapping agents for heteroatom and hydrocarbon peroxides.^{40–46} Thus, we hypothesized that O-transfer of the peroxy intermediate to (MeO)₃P will occur in the photoreaction of 1, as we observe. The photolysis of 1 with (MeO)₃P and ¹⁸O₂ led to ¹⁸O-labeled phosphate [(MeO)₃P=¹⁸O], indicating that the oxygen atom transferred to phosphite originated from ¹⁸O₂. Table 2 shows that the O atom transfer was dependent on the concentration of (MeO)₃P but not 1. That is, the yield of (MeO)₃P=O increased from 1.5 to 7.5 mM when the initial (MeO)₃P concentration increased from 20 to 60 mM. In contrast, the formation of (MeO)₃P=O remained constant at ~1.3–1.5 mM when the concentration of 1 increased from 20 to 60 mM. Trimethylphosphite is capable of trapping the peroxy intermediate and is relatively unreactive to the nitrosamine and oxygen reagents as well as the nitramine product. Control experiments showed that the yield of (MeO)₃P=O was 7-fold greater in the photoreaction of 1 with O₂ compared to a thermal reaction of (MeO)₃P with nitramine 3 after 1 h. Similarly, a literature report showed that a nitro compound was reduced to a nitroso compound with triethylphosphite.⁴⁷ The results of other control reactions also demonstrate that (i) the photolysis of (MeO)₃P itself with O₂ did not form (MeO)₃P=O (or only a minute amount formed: precision = ± 0.1%), (ii) nitramine 3 was not observed under the anaerobic photolysis of nitrosamine 1, and (iii) ¹⁸O from H₂¹⁸O did not photochemically exchange with nitrosamine.¹⁰

Trapping of the Peroxy Intermediate with Triphenylphosphine (Ph₃P) in the Dark. Phosphines have been

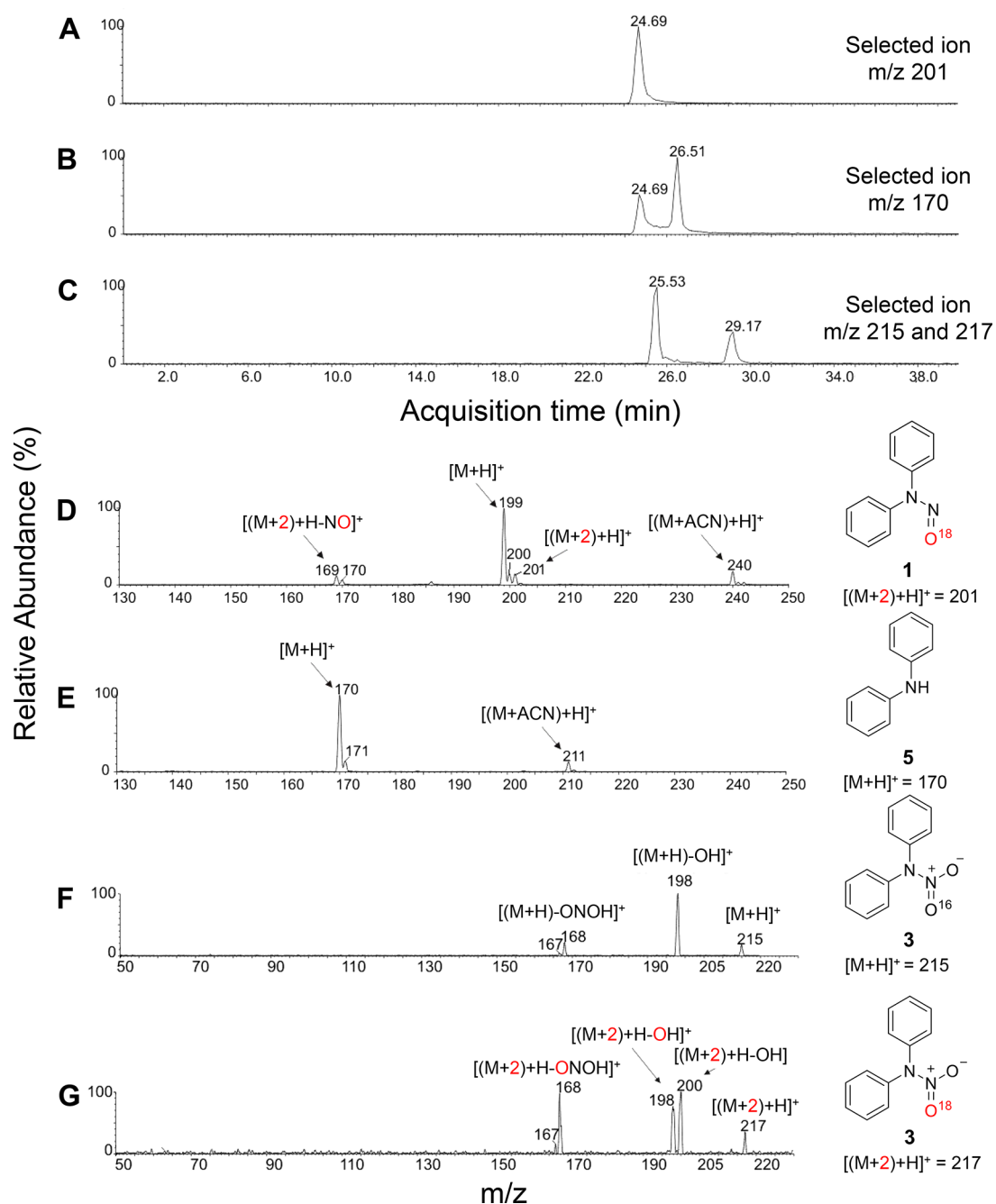


Figure 5. HPLC-MS/MS of products formed after 3 h photolysis of nitrosamine **1** with $^{18}\text{O}_2$ in chloroform. Ion-selection analysis for (A) ^{18}O -labeled nitrosamine **1** ($m/z = 201$), (B) Ph_2NH **5** ($m/z = 170$), (C) nitramine **3** ($m/z = 215$) and ^{18}O -labeled nitramine **3** ($m/z = 217$). MS/MS fragmentation of peak for (D) ^{18}O -labeled nitrosamine **1** at 24.69 min, (E) Ph_2NH **5** at 26.51 min, (F) unlabeled nitramine **3** at 25.53 min, and (G) ^{18}O -labeled nitramine **3** at 25.53 min. The peaks at 24.69 min in (B) and 29.17 min in (C) are unidentified products.

reported as powerful reducing agents of organic peroxides.^{48–50}

Thus, we examined whether the O-transfer of the peroxy intermediate to triphenylphosphine, Ph_3P , occurs upon low-temperature photooxidation of **1**, which is observed. The photolysis of nitrosamine **1** with O_2 was conducted in CH_2Cl_2 at $-90\text{ }^\circ\text{C}$. Here, O_2 was bubbled into the solution during the irradiation with a UV pen light. Immediately after the photolysis, Ph_3P was added to the reaction mixture in the dark in a substoichiometric amount. GCMS data showed that the amount of $\text{Ph}_3\text{P}=\text{O}$ was 4% in CH_2Cl_2 . Control photochemical experiments with Ph_3P and O_2 showed some formation of $\text{Ph}_3\text{P}=\text{O}$, demonstrating that Ph_3P can only be

used as a trap in the dark. To further study the reaction at a low temperature, chemiluminescence was discovered in the decomposition of the peroxy intermediate, which sheds light on the reaction mechanism.

Based on the above phosphite and phosphine trapping data, the peroxy intermediate forms in a 4–13% yields in the reaction.

Low-Level Chemiluminescence of Visible Light by Excited Species. Chemiluminescence has been used in the past as evidence for excited species,^{51,52} which we find in our reaction upon the thermal decomposition of the peroxy intermediate. Here, we find that in the presence of O_2 , a

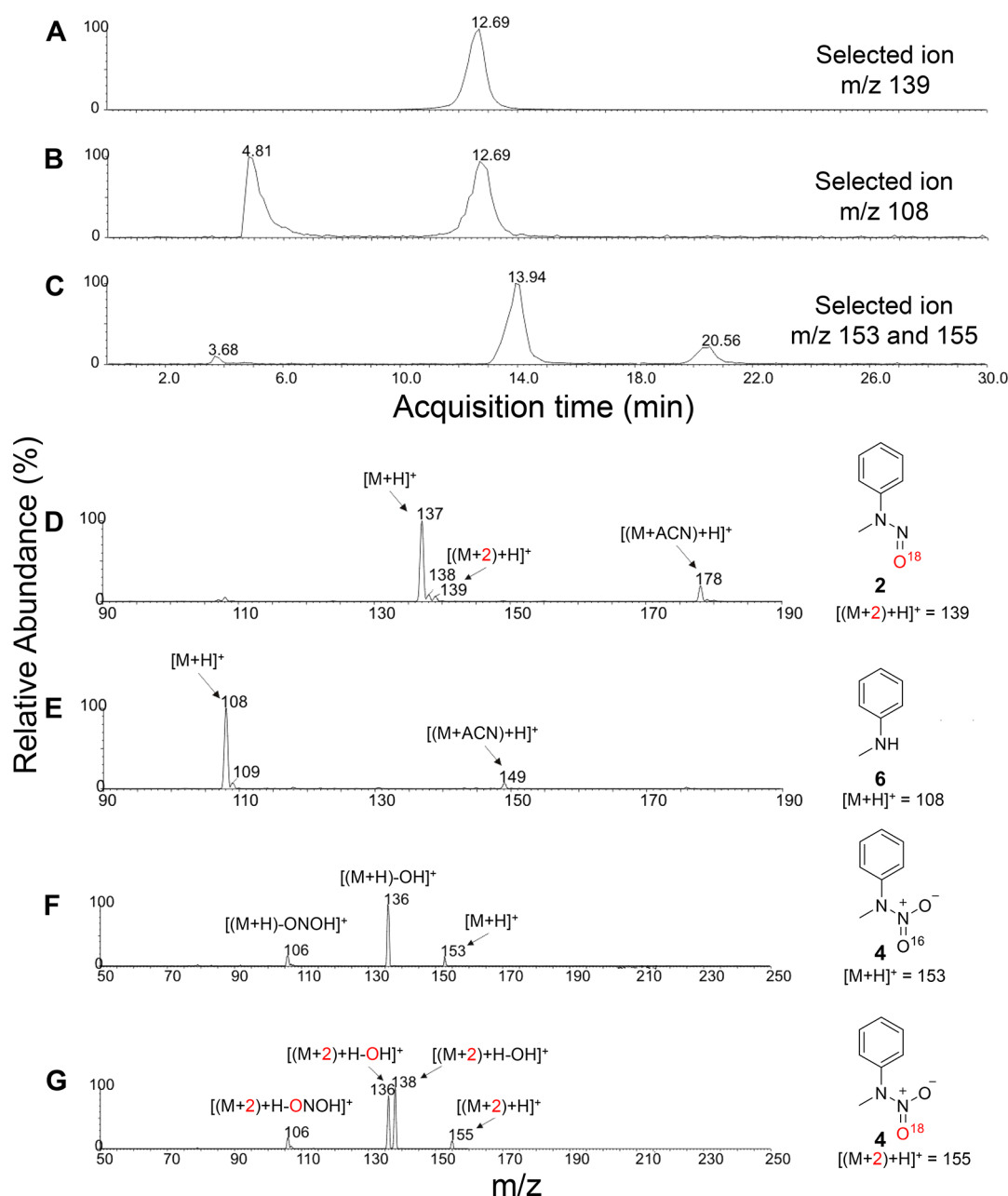


Figure 6. HPLC-MS/MS of products formed after 3 h photolysis of nitrosamine **2** with $^{18}\text{O}_2$ in chloroform. Ion-selection analysis for (A) ^{18}O -labeled nitrosamine **2** ($m/z = 139$), (B) *N*-methylaniline **6** ($m/z = 108$), (C) nitramine **4** ($m/z = 153$), and ^{18}O -labeled nitramine **4** ($m/z = 155$). MS/MS fragmentation of peak for (D) ^{18}O -labeled nitrosamine **2** at 12.69 min, (E) *N*-methylaniline **6** at 12.69 min, (F) unlabeled nitramine **4** at 13.94 min, and (G) ^{18}O -labeled nitramine **4** at 13.94 min. The peak at 4.81 min in (B) and 20.56 min in (C) are unidentified products.

peroxy intermediate is photochemically formed and produces chemiluminescence in the dark. The photolysis of **1** with a UV pen light and with O_2 bubbling was carried out at -72°C in CH_2Cl_2 for 5 min, and then the sample at -72°C was moved to the dark. Figure 8 shows a weak chemiluminescence emission detected in the visible region when the shutter door is opened at 0.5 min (black trace). The zero to 0.5 min period is the background of PMT, and from 0.5 min onward the chemiluminescence of the sample is recorded. We attribute the oscillations in the light emission to condensation because the temperature increases from -72 to 22°C over the course of the 8 min measurement. When the photoreaction is sparged with N_2 , the chemiluminescence is reduced significantly (Figure S5, Supporting Information), where not all O_2 is removed, and thus

a minor chemiluminescence is observed. When activator compounds 9,10-diphenylanthracene (DPA, blue trace) or 9,10-dibromoanthracene (DBA, red trace) are present, energy is transferred to them from the excited species generated upon decomposition of the peroxy intermediate. These results are reminiscent of previous reports^{53–56} of DPA- and DBA-enhanced chemiluminescence for evidence of excited-state ketones. The chemiluminescence data reported here and use of $(\text{MeO})_3\text{P}$ and Ph_3P as trapping reagents in the above sections point to the existence of a peroxy intermediate, which has been studied with DFT calculations (described next).

A question arose to us: What is the possible structure of the peroxy intermediate? Figure 9 shows conceivable structures for the peroxy intermediate, including *O*-nitrooxide diradical **A**

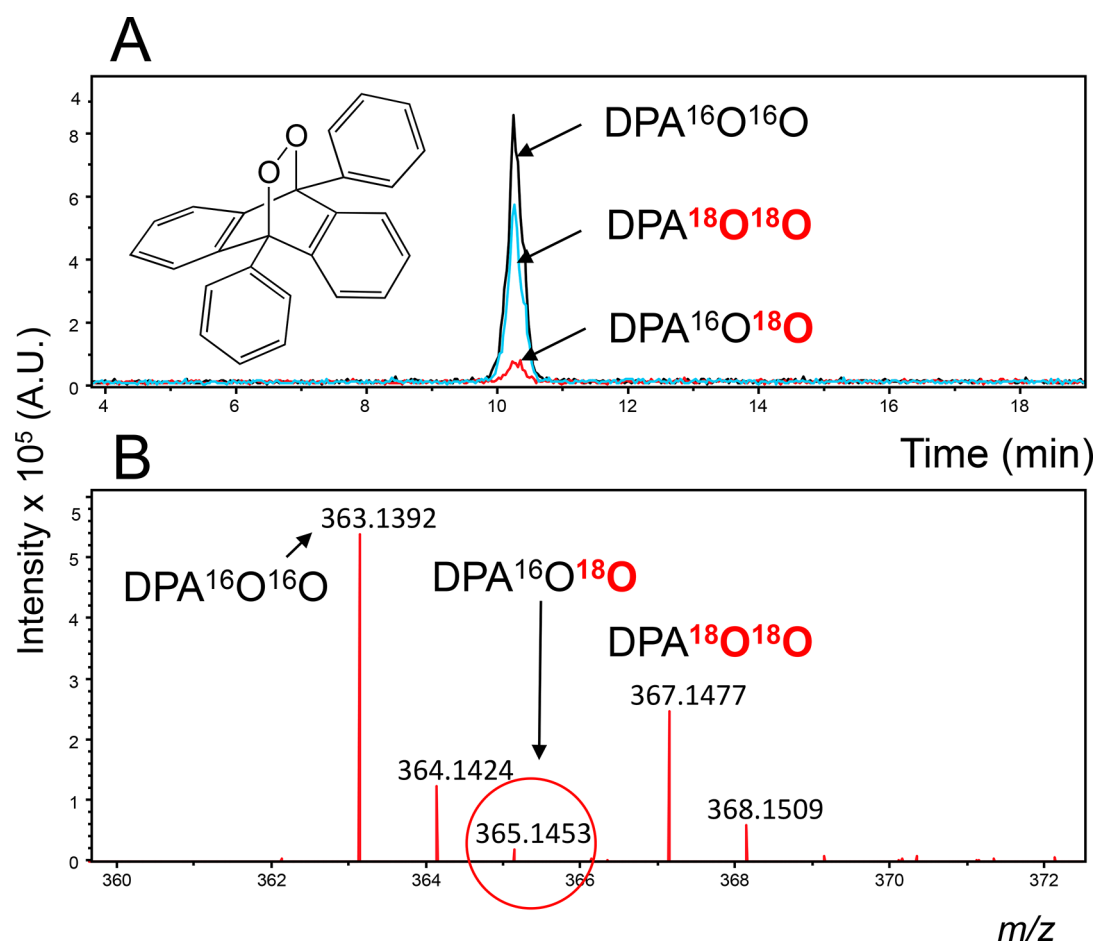


Figure 7. Trapping of $^{18}\text{O}=\text{}^{16}\text{O}$ expelled gas from a postphotolysis reaction of nitrosamine **1** with ^{18}O -labeled oxygen. (A) HPLC traces of DPA $^{16}\text{O}^{16}\text{O}$, DPA $^{16}\text{O}^{18}\text{O}$, and DPA $^{18}\text{O}^{18}\text{O}$ same retention time. (B) Mass spectra of the three anthracene endoperoxides.

Table 2. UV Photoreaction of $^{16}\text{O}_2$ and Nitrosamine **1**: Yields of Oxidized Trapping Agents Present during the Photolysis or Added after Photolysis in the Dark

nitrosamine 1 (mM)	trap	trap (mM)	yield of oxidized trap after 1 h irradiation ^{a,b}	
			(MeO) ₃ P=O (mM)	(MeO) ₂ P=O (%)
20	(MeO) ₃ P	20	1.5 ^a	7
20	(MeO) ₃ P	40	5.0 ^a	12
20	(MeO) ₃ P	50	6.7 ^a	13
20	(MeO) ₃ P	60	7.5 ^a	13
40	(MeO) ₃ P	20	1.4 ^a	7
60	(MeO) ₃ P	20	2.3 ^a	6

nitrosamine 1 (mM)	trap	trap (mM)	yield of oxidized trap after 1 h irradiation ^{c,d}	
			Ph ₃ P=O (mM)	Ph ₃ P=O (%)
1	Ph ₃ P	0.5	0.02	4

^aDetected by ^1H NMR spectroscopy. ^bControl experiments demonstrate that the aerobic UV irradiation of (MeO)₃P does not form (MeO)₃P=O in the absence of nitrosamine. Control experiments show that 0 mM and ~0.2 mM of (MeO)₃P=O arise from the thermal deoxygenation of nitrosamine **1** and nitramine **3**, respectively. ^cDetected by GCMS using biphenyl as the internal standard. ^dControl experiments show that Ph₃P does not deoxygenate nitrosamine **1**, and only deoxygenates nitramine **3** to a minor extent (<0.5%).

[R₂NN(-O[•])OO[•]], O-nitroxide zwitterion **B** [R₂NN⁺(=O)OO⁻], O-trioxidanyl diradical species **C** [R₂NN[•]OOO[•]], O-trioxidanyl zwitterion species **D** [R₂N⁺=NOOO⁻], 1,2,3,4-trioxazetidine **E** [cyclo-R₂NNO₃], 1,2,3,5,6-tetraoxadiazinane **F**, and 1,2,3,5,6,7,8-hexaoxadiazocane **G**.

DFT Computational Evidence for the Peroxy Intermediate. Figure 10 shows the ωb97x-D/6-311+G(d,p) calculated S₀ geometries of **A**, **B**, and **D–G**. Structures **C** and **D** do not optimize to minima and are instead second-order saddle points on the S₀ surface. The structures of the cyclic peroxides were optimized with nonequivalent N–O bond lengths: compare **E** (1.49 Å) with **F** (1.37 Å), and **G** (1.26 Å). Interestingly, one of the O–O bond lengths in **G** (1.69 and 1.31 Å) is considerably longer than the O–O bond length in **E** (1.43 Å), **F** (1.45 Å), and **B** (1.33 Å).

Figure 11 provides support for the idea that the nitroxide exists as a zwitterion **B** and not a diradical **A**. Unrestricted ωb97x-D/6-311+G(d,p) calculations show that there is no spin density for singlet nitroxide. That the nitroxide is a zwitterion is also supported by natural bonding orbital (NBO) calculations, where N(2) has a positive charge of +0.580, and O(3) has a negative charge of -0.438, in which polar structures are in general more stable as zwitterionic species than as diradical species.⁵⁷ Frontier molecular orbital (FMO) calculations (Figure 12) show that the highest occupied molecular orbital (HOMO) of **B** with two nonbonding orbitals is localized on N(1) and O(3). Both the lobes have *p*-character

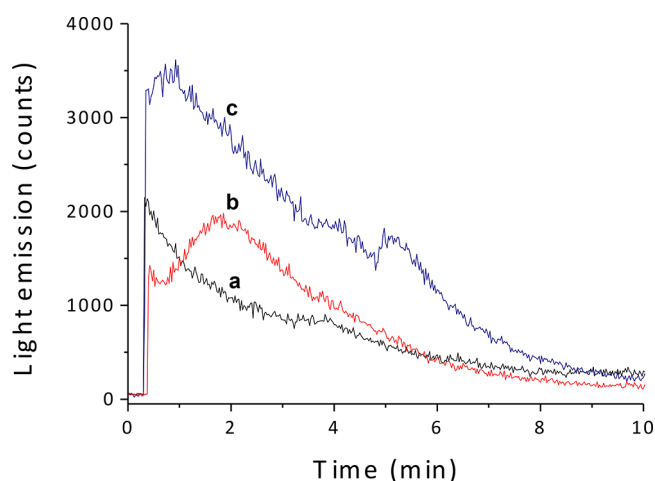


Figure 8. The UV–visible light emission by excited species produced in post-UV irradiated samples of nitrosamine 1 (5 mM) in CH_2Cl_2 at -72°C . After 30 seconds, the PMT window is opened, and the chemiluminescence of the sample was recorded. (a) Black trace: The sample was sparged with O_2 and then irradiated. After irradiation, the chemiluminescence was detected at room temperature. (b) Red trace: The sample was sparged with O_2 and then irradiated. After irradiation, 9,10-dibromoanthracene (DBA, 5 mM) was added to the reaction in the dark, and the chemiluminescence was detected at room temperature. All the traces were recorded in the dark. (c) Blue trace: The sample was sparged with O_2 and then irradiated. After irradiation, 9,10-diphenylanthracene (DPA, 5 mM) was added to the reaction in the dark, and the chemiluminescence was detected at room temperature. The spectral response range is from 185 nm to 900 nm, with peak sensitivity at 450 nm. At 450 nm, the detector's photocathode has a radiant sensitivity of 90 mA/W and a quantum efficiency of 24.8%.

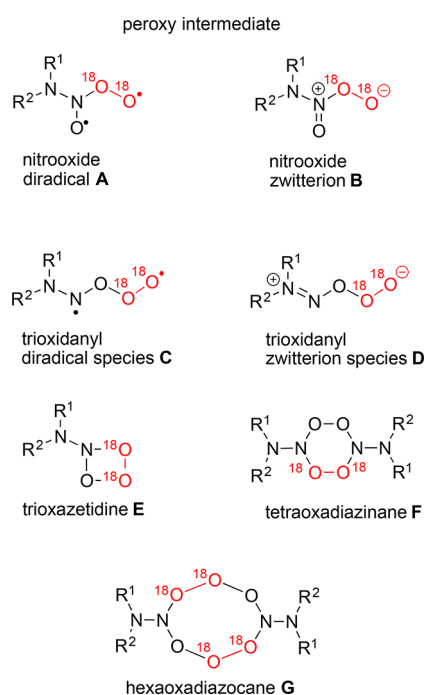


Figure 9. Possible structures of peroxy intermediates formed by the photooxidation of nitrosamines.

and show the presence of a lone pair of electrons as would be expected of zwitterionic **B** and not diradical **A**.

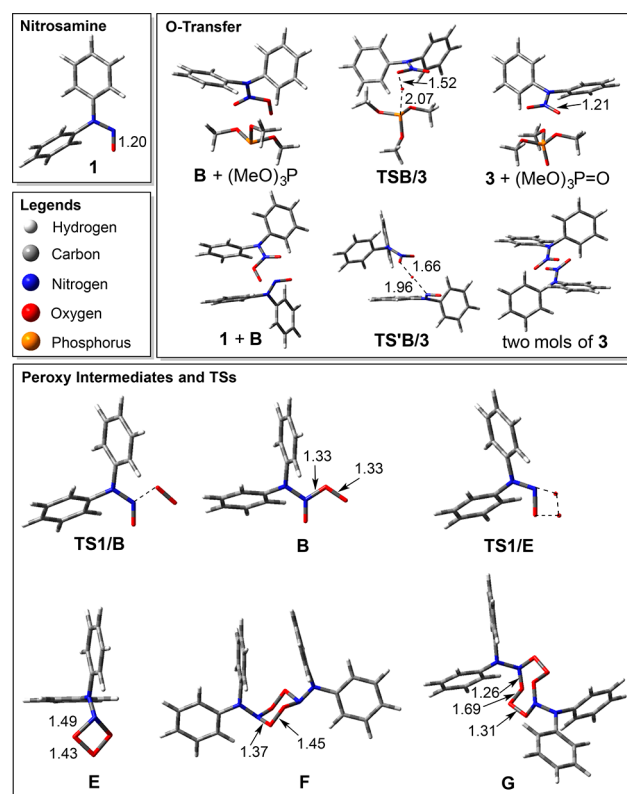


Figure 10. DFT calculations of peroxy species and transition structures (TSs).

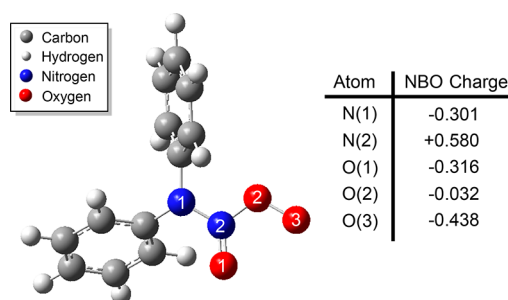


Figure 11. Computed NBO charges on the nitrogen and oxygen atoms of intermediate B.

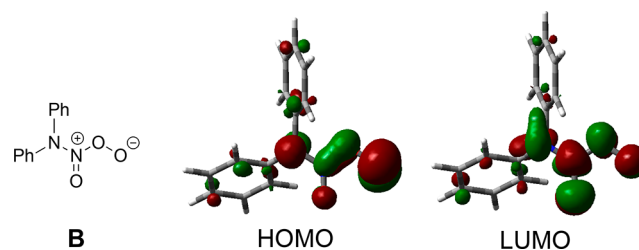


Figure 12. Computed FMOs of intermediate B, in which the positive isovalues are in red, and the negative isovalues are in green. Isovalue = 0.04.

TD-DFT calculations were also carried out with unrestricted $\omega\text{b97x-D}/6\text{-311+G(d,p)}$ calculations, along with the Tamm–Dancoff approximation (TDA)³⁹ due to possible triplet (T_1) instabilities.³⁸ The $S_0\text{-}S_1$ and $S_0\text{-}T_1$ energy gaps shown in Figure 13 are the vertical excitation energies. Figure 13 shows that nitrosamine 1 has a $S_0\text{-}S_1$ gap of 76.4 kcal/mol and a $S_0\text{-}$

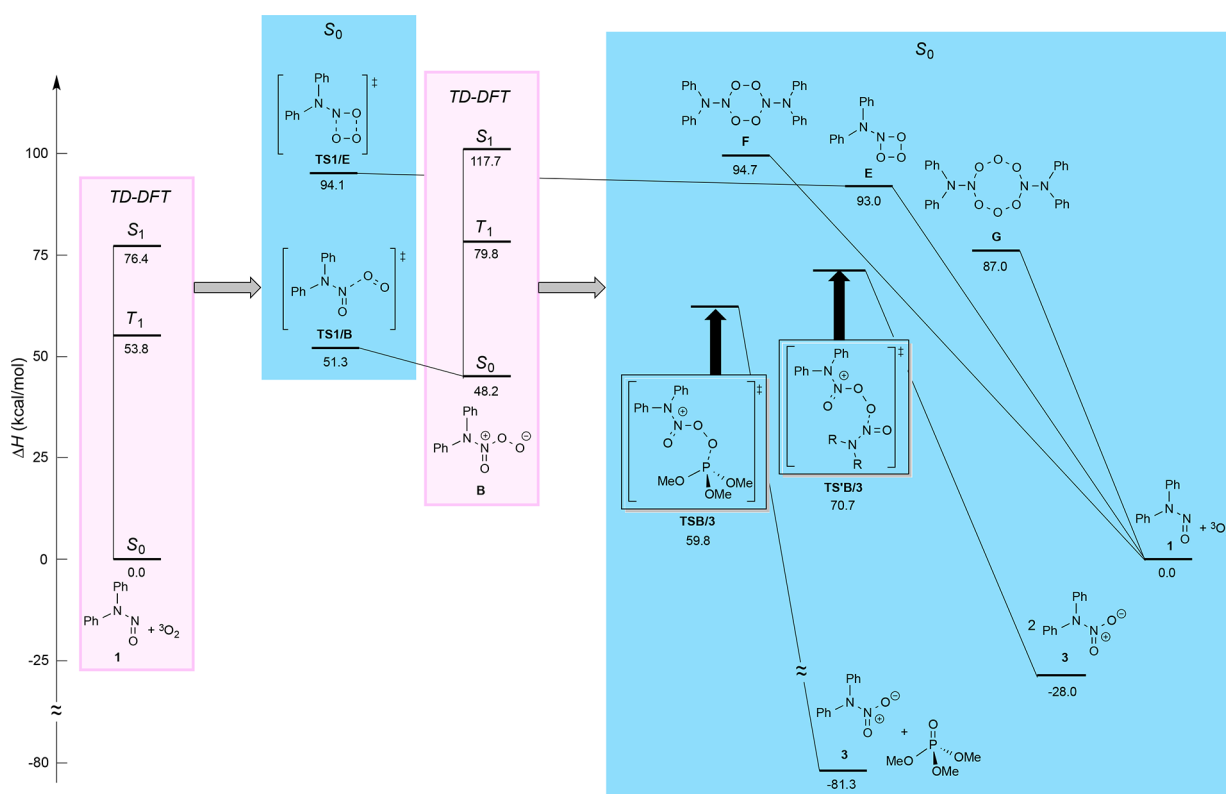


Figure 13. Computed surfaces showing the results of ground state DFT and TD-DFT calculations using ω b97x-D/6-311+G(d,p). The TD-DFT calculations employed the Tamm–Dancoff approximation, and the energy gaps for **1** and **B** represent the vertical excitation energies. Relative enthalpies (ΔH) are given in kcal/mol.

T_1 gap of 53.8 kcal/mol. These computed vertical energies are reminiscent of the experimental relaxed S_1 and T_1 energies reported for *N*-nitrosodimethylamine (72–73 kcal/mol and 58–59 kcal/mol, respectively).¹⁴ The experimental relaxed triplet excited-state energy of nitrosamine **1** has not been reported. Next, we calculated the vertical S_1 and T_1 energies of nitrooxide intermediate **B**. For **B**, the S_0 – S_1 gap is 69.5 kcal/mol and the S_0 – T_1 gap is 31.6 kcal/mol. The resulting spin densities on **B** were 0.0 on all atoms at both the S_1 and T_1 states, thus providing further evidence that the nitrooxide intermediate exists as a zwitterionic species rather than a diradical species. We note that our attempted optimization of triplet peroxy intermediates **A**–**G** resulted in their dissociation to nitrosamine **1** and $^3\text{O}_2$. The start guess structures for **A**–**G** were generated from singlet ground state (stable forms) except for **C** and **D**, which do not exist on the singlet surface. When **C** and **D** were optimized on the T_0 surface initially with the bond distance of ^{16}O – ^{18}O constrained at 1.32 Å, a subsequent unconstrained optimization of **C** and **D** led to the dissociation of $^3\text{O}_2$.

Figure 13 shows **1** and O_2 and peroxy species in relation to excited state energies. The interconversion of **1** and O_2 to reach **B** is a high-energy process ($\Delta H^\ddagger = 51.3$ kcal/mol and $\Delta H_{\text{rel}} = 48.2$ kcal/mol) and would require photoexcitation. On the basis of the DFT data, we propose the structure of the peroxy intermediate to be initially **B**. Figure 14 shows that the activation energy (ΔH^\ddagger) for O-transfer from **B** to $(\text{MeO})_3\text{P}$ is 11.6 kcal/mol, and $\Delta H_{\text{rel}} = -129.5$ kcal/mol. In contrast, the activation energy for O-transfer from **B** to **1** is higher in energy ($\Delta H^\ddagger = 22.5$ kcal/mol and $\Delta H_{\text{rel}} = -76.2$ kcal/mol). However, paths to cyclic peroxides are too high to be reached thermally

and would require photoexcitation. Thus, the proposed interconversion of intermediates in Figure 13 is uncertain at present. In contrast, our experimental data clearly provide evidence for the existence of a peroxy intermediate (vide supra), although its structure is uncertain at present. Based on our experimental data, the peroxy intermediate in the nitrosamine– $^3\text{O}_2$ photoreaction is less reactive compared to carbonyl oxide^{58–61} and nitroso-*O*-oxide^{62–66} that appear in ozonolysis and triplet nitrene– $^3\text{O}_2$ reactions, respectively, due to the latter's ability to oxidize solvents such as toluene.⁶⁷

In summary, the photolysis of nitrosamine with $^{18}\text{O}_2$ leads to the formation of a peroxy intermediate. Our new findings are as follows: (i) ^{18}O -labeled nitrosamines **1** and **2**, and ^{18}O -labeled nitramines **3** and **4** are formed as products. (ii) An oxygen atom is transferred to form the nitramine product. (iii) An oxygen atom is also transferred to a $(\text{MeO})_3\text{P}$ or Ph_3P trap. Experimental data show evidence for the existence of a peroxy intermediate. For example, Table 2 shows that the peroxy intermediate in the reaction can be trapped with $(\text{MeO})_3\text{P}$, or with Ph_3P in the dark (after the photolysis at a low temperature). Furthermore, the yield of the peroxy intermediate is 4–13% based on our trapping experiments. The peroxy intermediate leads to excited species and chemiluminescence (Figure 15). The thermal decomposition of the peroxy intermediate is attributed to the production of excited species similar to 1,2-dioxetanes reported in the literature.^{68–72} Although there is yet no spectroscopic evidence for **E** or **G**, they are notable owing to their structural similarity to 1,2-dioxetanes and cyclic organosilicon peroxides, respectively, which have been proposed.^{73–79} Our DFT calculations

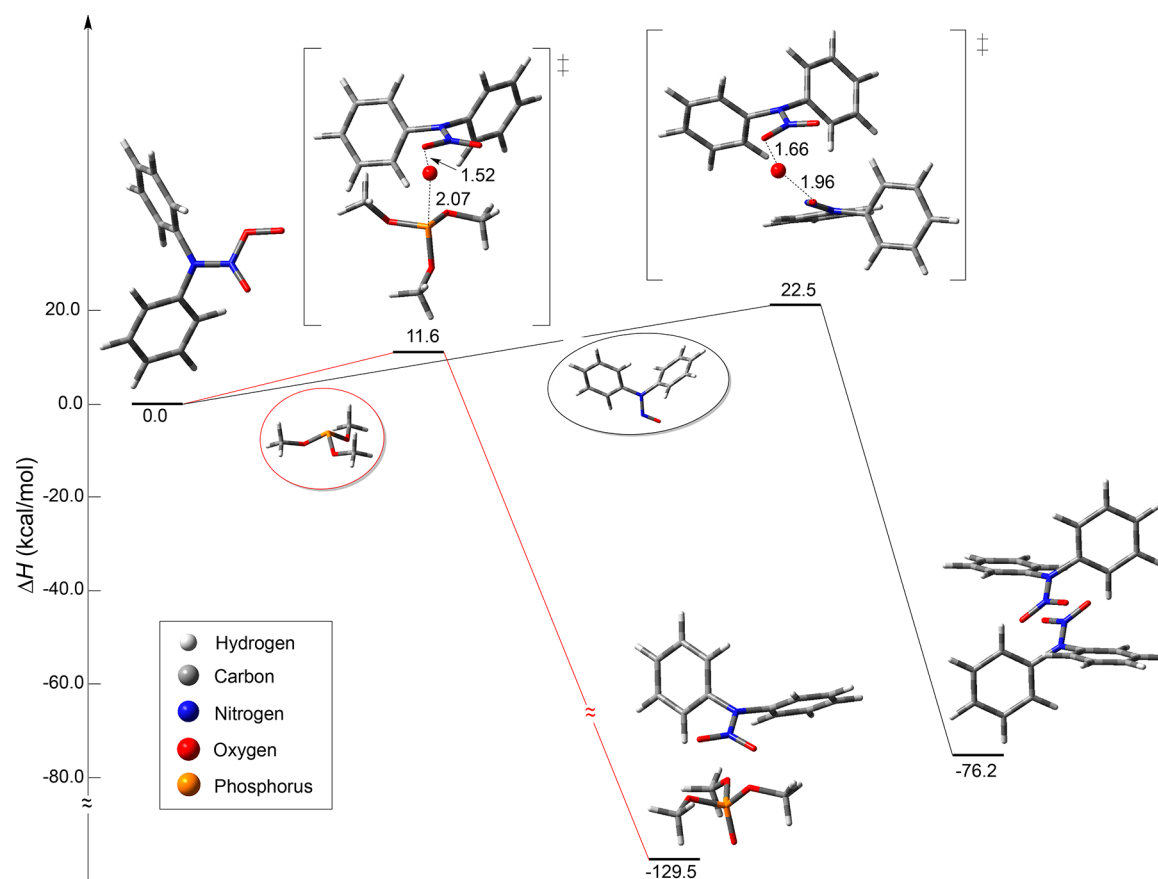


Figure 14. $U\omega b97x-D/6-311+G(d,p)$ computed potential energy surfaces for the O atom transfer reactions. The red line follows the O-transfer between **B** and $(MeO)_3P$ to reach **3** and $(MeO)_3P=O$, and the black line follows the O-transfer between **B** and **1** to reach two moles of **3**. Distances are given in Å. Energies are given in kcal/mol.

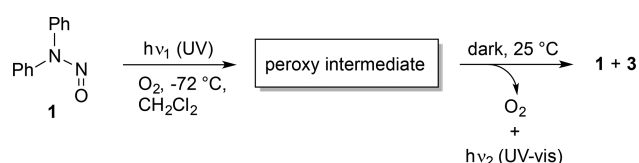


Figure 15. Proposed mechanism in which chemiluminescence arises by the initial formation of a peroxy intermediate followed by its decomposition.

tentatively predict an initial formation of nitroxide **B**, followed by ring closure to reach **E** or dimerize to reach **G**.

4. CONCLUSION

The results here show the utility of using isotopically labeled oxygen in a photooxidation reaction to gain insight into the mechanism. Our work relied on the photolysis of **1** and **2** in the presence of $^{18}O_2$ to produce ^{18}O -labeled nitrosamines **1** and **2**, and ^{18}O -labeled nitramines **3** and **4**. The current work shows nitrosamines in oxygen-transfer processes. Our previous work¹⁰ showed that nitrosamines are an oxygen carrier platform. The former is a photooxygen cycling process where some nitrosamines are regenerated by the reversible binding of O_2 . Further studies could include the synthesis of ^{15}N -labeled nitrosamines so that structural elucidation of the peroxy intermediate by ^{15}N NMR spectroscopy is possible. Also, the creation of a “persistent” peroxy intermediate by stabilizing it kinetically with sterically hindered groups to shield the peroxide groups would be useful as has been done with dioxaphosphir-

anes^{80–82} and carbonyl oxides⁸³ that were otherwise difficult to characterize. Further studies could also focus on the peroxy intermediate and its implications in biological toxicity and environmental fate of nitrosamines.

■ ASSOCIATED CONTENT

Supporting Information

The Supporting Information is available free of charge on the ACS Publications website at DOI: 10.1021/acs.jpca.7b02414.

HPLC/MS of products from the photooxidation of nitrosamine **1**, DFT computed geometries of all stationary points, and absolute energies (PDF)

■ AUTHOR INFORMATION

Corresponding Authors

*E-mail: Edyta.Greer@baruch.cuny.edu.

*E-mail: pdmascio@iq.usp.br.

*E-mail: agreer@brooklyn.cuny.edu.

ORCID

Alexander Greer: 0000-0003-4444-9099

Notes

The authors declare no competing financial interest.

■ ACKNOWLEDGMENTS

A.A.G., C.D., M.S.O., I.A. and A.G. acknowledge support from the National Science Foundation (CHE-1464975). E.M.G. and K.K. acknowledge support from the donors of the Petroleum

Research Fund of the American Chemical Society. Computational support was provided by the Extreme Science and Engineering Discovery Environment (XSEDE), which is supported by the National Science Foundation Grant No. ACI01053575. M.S.O., F.M. and P.D.M. acknowledge support from FAPESP (Fundação de Amparo à Pesquisa do Estado de São Paulo; No. 2012/12663-1, 2011/10048-5 and 2010/50891-0), CEPID Redoxoma (FAPESP; No. 2013/07937-8), CNPq (Conselho Nacional para o Desenvolvimento Científico e Tecnológico No. 301307/2013-0 and No. 159068/2014-2) and PRPUSP (Pro-Reitoria de Pesquisa da Universidade de São Paulo, NAP Redoxoma, No. 2011.1.9352.1.8). A.G. acknowledges support from a Tow Professorship at Brooklyn College. We thank Flavia Barragán, Leda Lee and Niluksha Walalawela for discussions.

REFERENCES

- Hecht, S. S.; Stepanov, I.; Carmella, S. G. Exposure and Metabolic Activation Biomarkers of Carcinogenic Tobacco-Specific Nitrosamines. *Acc. Chem. Res.* **2016**, *49*, 106–114.
- Lee, C.-F.; Krasner, S. W.; Scimmenti, M. J.; Prescott, M.; Guo, Y. C. Nitrosamine Precursors and Wastewater Indicators in Discharges in the Sacramento-San Joaquin Delta. In *Recent Advances in Disinfection By-Products*; Karanfil, T., Mitch, B., Westerhoff, P., Eds.; ACS Symposium Series, Vol. 1190; American Chemical Society: Washington, DC, 2015; Chapter 7, pp 119–133.
- Wink, D. A.; Nims, R. W.; Saavedra, J. E.; Desrosiers, M. F.; Ford, P. C. Oxidation of Alkyl Nitrosamines via the Fenton Reagent. Use of Nitrosamines to Probe Oxidative Intermediates in the Fenton Reaction. In *Nitrosamines and Related N-Nitroso Compounds*; Loepky, R. N., Michejda, C. J., Eds.; ACS Symposium Series, Vol. 553; American Chemical Society: Washington, DC, 1994; Chapter 30, pp 324–327.
- Yang, L.; Chen, Z.; Shen, J.; Xu, Z.; Liang, H.; Tian, J.; Ben, Y.; Zhai, X.; Shi, W.; Li, G. Reinvestigation of the Nitrosamine-Formation Mechanism During Ozonation. *Environ. Sci. Technol.* **2009**, *43*, 5481–5487.
- Dai, N.; Mitch, W. A. Controlling Nitrosamines, Nitramines, and Amines in Amine-based CO₂ Capture Systems with Continuous Ultraviolet and Ozone Treatment of Washwater. *Environ. Sci. Technol.* **2015**, *49*, 8878–8886.
- Mezyk, S. P.; Ewing, D. B.; Kiddle, J. J.; Madden, K. P. Kinetics and Mechanisms of the Reactions of Hydroxyl Radicals and Hydrated Electrons with Nitrosamines and Nitramines in Water. *J. Phys. Chem. A* **2006**, *110*, 4732–4737.
- Bunkan, A. J. C.; Hetzler, J.; Mikoviny, T.; Wisthaler, A.; Nielsen, C. J.; Olzmann, M. The Reactions of N-methylformamide and N,N-dimethylformamide with OH and Their Photo-Oxidation Under Atmospheric Conditions: Experimental and Theoretical Studies. *Phys. Chem. Chem. Phys.* **2015**, *17*, 7046–7059.
- Tang, Y.; Nielsen, C. J. Theoretical Study on the Formation and Photolysis of Nitrosamines (CH₃CH₂)NHNO and (CH₃CH₂)₂NNO under Atmospheric Conditions. *J. Phys. Chem. A* **2013**, *117*, 126–132.
- Karaki, F.; Kabasawa, Y.; Yanagimoto, T.; Umeda, N.; Urano, Y.; Nagano, T.; Otani, Y.; Ohwada, T. Visible-light-triggered Release of Nitric Oxide from N-pyramidal Nitrosamines. *Chem. - Eur. J.* **2012**, *18*, 1127–1141.
- Silva Oliveria, M.; Ghogare, A. A.; Abramova, I.; Greer, E. M.; Manso Prado, F.; Di Mascio, P.; Greer, A. Mechanism of Photochemical O-Atom Exchange in Nitrosamines with Molecular Oxygen. *J. Org. Chem.* **2015**, *80*, 6119–6127.
- Chow, Y. L.; Lau, M. P.; Cessna, A. J.; Yip, R. W. Flash Photolysis of N-nitrosopiperidine. Reactive Transient. *J. Am. Chem. Soc.* **1971**, *93*, 3808–3809.
- Mojelsky, T.; Chow, Y. L. Photoreactions of Nitroso Compounds in Solution. XXVII. Polar Effects of the Aminium Radical Addition to Styrenes. *J. Am. Chem. Soc.* **1974**, *96*, 4549–4554.
- Perry, R. A.; Lockhart, R. W.; Kitadani, M.; Chow, Y. L. Syntheses of Azapolycyclic Compounds by Aminium Radical Routes: Trapping of the Radical Intermediates. *Can. J. Chem.* **1978**, *56*, 2906–2913.
- Chow, Y. L.; Wu, Z.-Z.; Lau, M.-P.; Yip, R. W. On the Singlet and Triplet Excited State of Nitrosamines. *J. Am. Chem. Soc.* **1985**, *107*, 8196–8201.
- Chow, Y. L. Nitrosamine Photochemistry. Reactions of Aminium Radicals. *Acc. Chem. Res.* **1973**, *6*, 354–360.
- Maruthamuthu, P.; Scaiano, J. C. Biradical Double Trapping by Nitric Oxide. An Electron Spin Resonance Study. *J. Phys. Chem.* **1978**, *82*, 1588–1591.
- Crumrine, D. S.; Brodbeck, C. M.; Dombrowski, P. H.; Haberkamp, T. J.; Kekstas, R. J.; Nabor, P.; Nomura, G. S.; Padleckas, H. A.; Suther, D. J.; Yonan, J. P. Photocleavage of Diarylnitrosamines in Neutral Media. *J. Org. Chem.* **1982**, *47*, 4246–4249.
- Piech, K.; Bally, T.; Sikora, A.; Marcinek, A. Mechanistic Aspects of the Oxidative and Reductive Fragmentation of N-nitrosamines: A New Method for Generating Nitrenium Cations, Amide Anions, and Aminyl Radicals. *J. Am. Chem. Soc.* **2007**, *129*, 3211–3217.
- Lymar, S. V.; Shafirovich, V. Photoinduced Release of Nitroxyl and Nitric Oxide from Diazeniumdiolates. *J. Phys. Chem. B* **2007**, *111*, 6861–6867.
- Ohwada, T.; Miura, M.; Tanaka, H.; Sakamoto, S.; Yamaguchi, K.; Ikeda, H.; Inagaki, S. Structural Features of Aliphatic N-Nitrosamines of 7-Azabicyclo[2.2.1]heptanes that Facilitate N–NO Bond Cleavage. *J. Am. Chem. Soc.* **2001**, *123*, 10164–10172.
- Bennett, J. E.; Howard, J. A. Bimolecular Self-Reaction of Peroxy Radicals. Oxygen 18 Isotope Study. *J. Am. Chem. Soc.* **1973**, *95*, 4008–4010.
- Clennan, E. L.; Yang, K. ¹⁷O Isotopic Tracer Evidence for the Formation of a Sulfurane Intermediate During Sulfide Photooxidation. *J. Am. Chem. Soc.* **1990**, *112*, 4044–4046.
- Savarino, J.; Thiemens, M. H. Mass-Independent Oxygen Isotope (¹⁶O, ¹⁷O, ¹⁸O) Fractionation Found in H₂O_x Reactions. *J. Phys. Chem. A* **1999**, *103*, 9221–9229.
- Smirnov, V. V.; Lanci, M. P.; Roth, J. P. Computational Modeling of Oxygen Isotope Effects on Metal-Mediated O₂ Activation at Varying Temperatures. *J. Phys. Chem. A* **2009**, *113*, 1934–1945.
- Ashley, D. C.; Brinkley, D. W.; Roth, J. P. Oxygen Isotope Effects as Structural and Mechanistic Probes in Inorganic Oxidation Chemistry. *Inorg. Chem.* **2010**, *49*, 3661–3675.
- Buchachenko, A. L.; Dubinina, E. O. Photo-oxidation of Water by Molecular Oxygen: Isotope Exchange and Isotope Effects. *J. Phys. Chem. A* **2011**, *115*, 3196–3200.
- Yeung, L. Y.; Okumura, M.; Zhang, J.; Minton, T. K.; Paci, J. T.; Karton, A.; Martin, J. M. L.; Camden, J. P.; Schatz, G. C. O(³P) + CO₂ Collisions at Hyperthermal Energies: Dynamics of Nonreactive Scattering, Oxygen Isotope Exchange, and Oxygen-Atom Abstraction. *J. Phys. Chem. A* **2012**, *116*, 64–84.
- Xu, W.-T.; Huang, B.; Dai, J.-J.; Xu, J.; Xu, H.-J. Catalyst-Free Singlet Oxygen-Promoted Decarboxylative Amidation of α -Keto Acids with Free Amines. *Org. Lett.* **2016**, *18*, 3114–3117.
- Civiš, S.; Bouša, M.; Zukal, A.; Knížek, A.; Kubelík, P.; Rojik, P.; Nováková, J.; Fergus, M. Spontaneous Oxygen Isotope Exchange between Carbon Dioxide and Oxygen-Containing Minerals: Do the Minerals “Breathe” CO₂? *J. Phys. Chem. C* **2016**, *120*, 508–516.
- Masslynx Mass Spectrometry Software; software available at <http://www.sisweb.com/mstools/isotope.htm> (accessed Feb 1, 2017).
- Daszkiewicz, Z.; Domański, A.; Kyzioł, J. B. An Alternate Method for the Synthesis of Secondary Nitramines. *Org. Prep. Proced. Int.* **1994**, *26*, 337–341.
- Frisch, M. J.; Trucks, G. W.; Schlegel, H. B.; Scuseria, G. E.; Robb, M. A.; Cheeseman, J. R.; Scalmani, G.; Barone, V.; Mennucci, B.; Petersson, G. A. et al. *Gaussian 09*, Revision D.01; Gaussian, Inc.: Wallingford, CT, 2009.
- Chai, J.-D.; Head-Gordon, M. Long-Range Corrected Hybrid Density Functionals with Damped Atom-Atom Dispersion Corrections. *Phys. Chem. Chem. Phys.* **2008**, *10*, 6615–6620.

- (34) Dennington, R.; Keith, T.; Millam, J. *Gaussview*; Semichem Inc.: Shawnee Mission, KS, 2009.
- (35) Saito, T.; Nishihara, S.; Kataoka, Y.; Nakanishi, Y.; Kitagawa, Y.; Kawakami, T.; Yamanaka, S.; Okumura, M.; Yamaguchi, K. Reinvestigation of the Reaction of Ethylene and Singlet Oxygen by the Approximate Spin Projection Method. Comparison with Multi-reference Coupled-Cluster Calculations. *J. Phys. Chem. A* **2010**, *114*, 7967–7974.
- (36) Fukui, K. A Formulation of Reaction Coordinate. *J. Phys. Chem.* **1970**, *74*, 4161–4163.
- (37) Fukui, K. The Path of Chemical Reactions—The IRC Approach. *Acc. Chem. Res.* **1981**, *14*, 363–368.
- (38) Cordova, F.; Doriol, L. J.; Ipatov, A.; Casida, M. E.; Filippi, C.; Vela, A. Troubleshooting Time-Dependent Density-Functional Theory for Photochemical Applications: Oxirane. *J. Chem. Phys.* **2007**, *127*, 164111.
- (39) Hirata, S.; Head-Gordon, M. Time-Dependent Density Functional Theory within the Tamm-Dancoff Approximation. *Chem. Phys. Lett.* **1999**, *314*, 291–299.
- (40) Miyamoto, S.; Martinez, G. R.; Medeiros, M. H. G.; Di Mascio, P. Singlet Molecular Oxygen Generated from Lipid Hydroperoxides by the Russell Mechanism: Studies Using ^{18}O -Labeled Linoleic Acid Hydroperoxide and Monomol Light Emission Measurements. *J. Am. Chem. Soc.* **2003**, *125*, 6172–6179.
- (41) Nahm, K.; Foote, C. S. Trimethyl Phosphite Traps Intermediates in the Reaction of Singlet Oxygen ($^1\text{O}_2$) and Diethyl Sulfide. *J. Am. Chem. Soc.* **1989**, *111*, 1909–1910.
- (42) Tsuji, S.; Kondo, M.; Ishiguro, K.; Sawaki, Y. Phosphadioxirane Intermediates in the Reaction of Singlet Oxygen with Phosphites and Phosphines. *J. Org. Chem.* **1993**, *58*, 5055–5059.
- (43) Poon, T. H. W.; Pringle, K.; Foote, C. S. Reaction of Cyclooctenes with Singlet Oxygen. Trapping of a Peroxide Intermediate. *J. Am. Chem. Soc.* **1995**, *117*, 7611–7618.
- (44) Sueishi, Y.; Miyake, Y. Spin Trapping of Phosphorus-Centered Radicals Produced by the Reactions of Dibenzoyl Peroxide with Organophosphorus Compounds. *Bull. Chem. Soc. Jpn.* **1997**, *70*, 397–403.
- (45) Clennan, E. L.; Stensaas, K. L.; Rupert, S. D. Trapping of Peroxidic Intermediates with Sulfur and Phosphorus Centered Electrophiles. *Heteroat. Chem.* **1998**, *9*, 51–56.
- (46) Oba, M.; Okada, Y.; Nishiyama, K.; Ando, W. Aerobic Photooxidation of Phosphite Esters Using Diorganotelluride Catalysts. *Org. Lett.* **2009**, *11*, 1879–1881.
- (47) Boulton, A. J.; Fletcher, I. J.; Katritzky, A. R. Trapping a Nitroso-Compound Formed by Reduction of a Nitro-Compound with Triethyl Phosphite. *Chem. Commun.* **1968**, 62a.
- (48) Harris, J. R.; Haynes, M. T., II; Thomas, A. M.; Woerpel, K. A. Phosphine-Catalyzed Reductions of Alkyl Silyl Peroxides by Titanium Hydride Reducing Agents: Development of the Method and Mechanistic Investigations. *J. Org. Chem.* **2010**, *75*, 5083–5091.
- (49) Bonesi, S. M.; Protti, S.; Albin, A. Reactive Oxygen Species (ROS)-vs Peroxyl-Mediated Photosensitized Oxidation of Triphenylphosphine: A Comparative Study. *J. Org. Chem.* **2016**, *81*, 11678–11685.
- (50) Beaver, B.; Rawlings, D.; Neta, P.; Alfassi, Z. B.; Das, T. N. Structural Effects on the Reactivity of Arylphosphines as Potential Oxygen-Scavenging Additives for Future Jet Fuels. *Heteroat. Chem.* **1998**, *9*, 133–138.
- (51) Nascimento, A. L. T. O.; Cilento, G. Generation of Electronically Excited States in Situ. Polymorphonuclear Leukocytes Treated with Phenylacetaldehyde. *Photochem. Photobiol.* **1987**, *46*, 137–141.
- (52) Cilento, G. Photobiochemistry Without Light. *Experientia* **1988**, *44*, 572–576.
- (53) Catalani, L. H.; Wilson, T. Electron Transfer and Chemiluminescence. Two Inefficient Systems: 1,4-Dimethoxy-9,10-diphenylanthracene Peroxide and Diphenoyl Peroxide. *J. Am. Chem. Soc.* **1989**, *111*, 2633–2639.
- (54) Catalani, L. H.; Wilson, T. Energy Transfer from Triplet Acetophenones to 9,10-Dibromoanthracene (S1): Role of its Tn State. *J. Am. Chem. Soc.* **1987**, *109*, 7458–7462.
- (55) Catalani, L. H.; Wilson, T.; Bechara, E. J. H. Two Water-soluble Fluorescence Probes for Chemiexcitation Studies: Sodium 9,10-Dibromo- and 9, 10-Diphenylanthracene-2-Sulfonate. Synthesis, Properties and Application to Triplet Acetone and Tetramethyldioxetane. *Photochem. Photobiol.* **1987**, *45*, 273–281.
- (56) Di Mascio, P.; Catalani, L. H.; Bechara, E. J. H. Are Dioxetanes Chemiluminescent Intermediates in Lipoperoxidation. *Free Radical Biol. Med.* **1992**, *12*, 471–478.
- (57) Salem, L. Transition States and Reaction Mechanisms in Organic Chemistry. *The New World of Quantum Chemistry*; Springer: Netherlands, Dordrecht, Holland, 1979; Vol 2, pp 241–269.
- (58) Kuwata, K. T.; Hermes, M. R.; Carlson, M. J.; Zogg, C. K. Computational Studies of the Isomerization and Hydration Reactions of Acetaldehyde Oxide and Methyl Vinyl Carbonyl Oxide. *J. Phys. Chem. A* **2010**, *114*, 9192–9204.
- (59) Mansergas, A.; Anglada, J. M. Reaction Mechanism between Carbonyl Oxide and Hydroxyl Radical: A Theoretical Study. *J. Phys. Chem. A* **2006**, *110*, 4001–4011.
- (60) Kroll, J. H.; Donahue, N. M.; Cee, V. J.; Demerjian, K. L.; Anderson, J. G. Gas-Phase Ozonolysis of Alkenes: Formation of OH from Anti Carbonyl Oxides. *J. Am. Chem. Soc.* **2002**, *124*, 8518–8519.
- (61) Fenske, J. D.; Hasson, A. S.; Paulson, S. E.; Kuwata, K. T.; Ho, A.; Houk, K. N. The Pressure Dependence of the OH Radical Yield from Ozone–Alkene Reactions. *J. Phys. Chem. A* **2000**, *104*, 7821–7833.
- (62) Talipov, M. R.; Khursan, S. L.; Safiullin, R. L. RRKM and *ab initio* Investigation of the NH (X) Oxidation by Dioxide. *J. Phys. Chem. A* **2009**, *113*, 6468–6476.
- (63) Chainikova, E. M.; Safiullin, R. L.; Spirikhin, L. V.; Abdullin, M. F. A Revised Mechanism of Thermal Decay of Arylnitroso Oxides. *J. Phys. Chem. A* **2012**, *116*, 8142–8147.
- (64) Chainikova, E. M.; Pankratyev, E. Y.; Teregulova, A. N.; Gataullin, R. R.; Safiullin, R. L. Thermal Intramolecular Transformation of Key Intermediates in the Photooxidation of *para*-Allyl-Substituted Phenyl Azide. *J. Phys. Chem. A* **2013**, *117*, 2728–2737.
- (65) Mieres-Pérez, J.; Mendez-Vega, E.; Velappan, K.; Sander, W. Reaction of Triplet Phenylnitrene with Molecular Oxygen. *J. Org. Chem.* **2015**, *80*, 11926–11931.
- (66) Yusupova, A. R.; Safiullin, R. L.; Khursan, S. L. Conformational Transformations in Aromatic Nitroso Oxides. *J. Phys. Chem. A* **2016**, *120*, 5693–5705.
- (67) Ishiguro, K.; Sawaki, Y. Structure and Reactivity of Amphoteric Oxygen Species. *Bull. Chem. Soc. Jpn.* **2000**, *73*, 535–552.
- (68) Horn, K. A.; Schuster, G. B. Electronic Excitation Energy Partitioning in Dissymmetric Dioxetane Thermolyses. The Absolute Chemiluminescence Yields and Triplet to Singlet Excited State Ratios for 3-Acetyl-4,4-dimethyl-1,2-dioxetane. *J. Am. Chem. Soc.* **1978**, *100*, 6649–6656.
- (69) Schmidt, S. P.; Schuster, G. B. Chemiluminescence of Dimethyldioxetane. Unimolecular Generation of Excited Singlet and Triplet Acetone. Chemically Initiated Electron-Exchange Luminescence, the Primary Light Generating Reaction. *J. Am. Chem. Soc.* **1980**, *102*, 306–314.
- (70) Quinga, E. M. Y.; Mendenhall, G. D. Chemiluminescence from Hyponitrite Esters. Excited Triplet States from Dismutation of Geminate Alkoxy Radical Pairs. *J. Am. Chem. Soc.* **1983**, *105*, 6520–6521.
- (71) De Vico, L.; Liu, Y.-J.; Krogh, J. W.; Lindh, R. Chemiluminescence of 1,2-Dioxetane. Reaction Mechanism Uncovered. *J. Phys. Chem. A* **2007**, *111*, 8013–8019.
- (72) Velosa, A. C.; Baader, W. J.; Stevani, C. V.; Mano, C. M.; Bechara, E. J. H. 1,3-Diene Probes for Detection of Triplet Carbonyls in Biological Systems. *Chem. Res. Toxicol.* **2007**, *20*, 1162–1169.
- (73) Bartlett, P. D.; Traylor, T. G. Reaction of Diphenyldiazomethane with Oxygen. The Criegee Carbonyl Oxide. *J. Am. Chem. Soc.* **1962**, *84*, 3408–3409.

(74) Srinivasan, A.; Kebede, N.; Saavedra, J. E.; Nikolaitchik, A. V.; Brady, D. A.; Yourd, E.; Davies, K. M.; Keefer, L. K.; Toscano, J. P. Chemistry of the Diazeniumdiolates. 3. Photoreactivity. *J. Am. Chem. Soc.* **2001**, *123*, 5465–5481.

(75) Ruane, P. H.; Bushan, K. M.; Pavlos, C. M.; D'Sa, R. A.; Toscano, J. P. Controlled Photochemical Release of Nitric Oxide from O^2 -benzyl-Substituted Diazeniumdiolates. *J. Am. Chem. Soc.* **2002**, *124*, 9806–9811.

(76) Pavlos, C. M.; Cohen, A. D.; D'Sa, R. A.; Sunoj, R. B.; Wasylenko, W. A.; Kapur, P.; Relyea, H. A.; Kumar, N. A.; Hadad, C. M.; Toscano, J. P. Photochemistry of 1-(*N,N*-Diethylamino)diazenium-1,2-diolate: An Experimental and Computational Investigation. *J. Am. Chem. Soc.* **2003**, *125*, 14934–14940.

(77) Gritsan, N. P. Study of Photochemical Transformations of Organic Azides by Matrix Isolation Techniques and Quantum. *Russ. Chem. Rev.* **2007**, *76*, 1139–1160.

(78) Sawwan, N.; Greer, A. Rather Exotic Types of Cyclic Peroxides: Heteroatom Dioxiranes. *Chem. Rev.* **2007**, *107*, 3247–3285.

(79) Arzumanyan, A. V.; Terent'ev, A. O.; Novikov, R. A.; Lakhtin, V. G.; Grigoriev, M. S.; Nikishin, G. I. Reduction of Organosilicon Peroxides: Ring Contraction and Cyclodimerization. *Organometallics* **2016**, *35*, 1667–1673.

(80) Ho, D. G.; Gao, R.; Celaje, J.; Chung, H.-Y.; Selke, M. Phosphadioxirane: A Peroxide from an Ortho-Substituted Arylphosphine and Singlet Dioxygen. *Science* **2003**, *302*, 259–262.

(81) Zhang, D.; Gao, R.; Afzal, S.; Vargas, M.; Sharma, S.; McCurdy, A.; Yousufuddin, M.; Stewart, T.; Bau, R.; Selke, M. Intramolecular Arene Epoxidation by Phosphadioxiranes. *Org. Lett.* **2006**, *8*, 5125–5128.

(82) Zhang, D.; Ye, B.; Ho, D. G.; Gao, R.; Selke, M. Chemistry of Singlet Oxygen with Arylphosphines. *Tetrahedron* **2006**, *62*, 10729–10733.

(83) Sander, W.; Kirschfeld, A.; Kappert, W.; Muthusamy, S.; Kiselewsky, M. Dimesitylketone *O*-Oxide: First NMR Spectroscopic Characterization of a Carbonyl *O*-Oxide. *J. Am. Chem. Soc.* **1996**, *118*, 6508–6509.